



Identification and Contagion Study of Price Bubbles in Bulk Nonferrous Metals

Yu Zhao^{1,2,a}, Juntao Zhang^{2,*}, Deqing Zeng^{2,b}

¹School of Economics and Management, East China University of Technology, Nanchang, 330013, China

²Resources and Environmental Economics Research Centre, East China University of Technology, Nanchang, 330013, China

^azhaoyu8210@126.com, ^{*}1904148823@qq.com

^b2486446009@qq.com

Abstract. Based on the daily price index samples of copper, aluminum, lead, zinc, and nickel in China from 2019 to 2023, this study employs the Backward Sup Augmented Dickey-Fuller test, R-Vine Copula model, Granger causality test, and vector autoregression model to investigate the statistical characteristics and contagion of price bubble risks in the domestic non-ferrous metal market. Additionally, the impact of the international geopolitical risk index on China's non-ferrous metal price bubbles is explored. The research findings indicate that significant price bubbles exist in the copper, aluminum, zinc, and nickel markets in China. The non-ferrous metal market price bubbles are predominantly long-lasting, with the price bubble risk ranked from largest to smallest as aluminum, copper, zinc, and nickel. Regarding the contagion of price bubble risks, a price bubble in the copper market leads to price bubbles in the aluminum, zinc, and nickel markets. International geopolitical risks have a positive impact on the price bubbles of copper and aluminum in China, with the impact peaking within six trading days and diminishing to zero after nine trading days.

Keywords: Nonferrous Metals; Price Bubbles; Price Risk; Backward Sup Augmented Dickey-Fuller.

1 Introduction

The prices of nonferrous metals are highly susceptible to fluctuations in the economic cycle, exhibiting strong volatility. Since 2019, events such as the COVID-19 pandemic, the Russia-Ukraine conflict, and unexpected monetary policies have significantly impacted the bulk nonferrous metals market, causing prices to deviate from their fundamental values and triggering price bubbles. Therefore, studying the statistical characteristics and contagion of price bubbles in the domestic bulk nonferrous metals market since 2019, and analyzing the impact of international geopolitical risks on these price bubbles, is beneficial for several reasons. It helps relevant departments improve the national reserve mechanism for commodities, the price bubble early warning system,

© The Author(s) 2024

K. Zhang et al. (eds.), *Proceedings of the 5th International Conference on Economic Management and Big Data Application (ICEMBDA 2024)*, Advances in Economics, Business and Management Research 313, https://doi.org/10.2991/978-94-6463-638-3_5

and market regulation mechanisms, thereby safeguarding national resource security. Moreover, it aids enterprises in optimizing procurement and inventory strategies, formulating hedging strategies, and mitigating price risks.

The literature on studying price bubbles in nonferrous metals using the BSADF method is relatively scarce. Existing research predominantly uses this method to measure price bubbles in financial assets, such as agricultural commodity futures price bubbles[1], cryptocurrency price bubbles[2], real estate price bubbles[3], and stock price bubbles[4]. There are also significant price bubbles in the markets for nonferrous metals such as copper, zinc, lead, and aluminum[5], highlighting the necessity of setting up warning standards based on price bubble characteristics and establishing real-time warning systems for the nonferrous metals market[6].

Current research mainly evaluates bubble risk through two indicators: the existence and duration of bubbles, with less focus on the contagion of bubbles. The main methodologies used include the VAR model[7], Granger causality tests[8], and the Spatial Durbin Model[9]. Moreover, studies on price risk contagion are primarily based on price differential data or asset return data, lacking research on risk contagion based on price bubble sequences. Using price bubble data to study risk contagion can better reveal the contagion mechanism of asset price bubbles[10].

Although existing literature provides substantial material and important references, this paper can make marginal contributions in the following areas: first, identifying the statistical characteristics of price bubble sequences in the nonferrous metals market using the BSADF method; second, analyzing risk contagion and impulse responses to external shocks based on price bubble sequences. The research results can provide references for monitoring and early warning of price bubble risks in the nonferrous metals market.

2 Model Introduction and Data Source

The measurement of price bubbles essentially involves identifying explosive price movements. Consider the generation process of nonferrous metal price data as shown in Equation (1):

$$P_t = dT^{-\eta} + \theta P_{t-1} + \varepsilon_t, \quad \varepsilon_t \sim i.i.d. N(0, \sigma^2) \quad (1)$$

Here, d is a constant, T represents the sample size, η is a locating coefficient controlling the magnitude of intercept and drift ($\eta > 0.5$), and ε_t is the error term satisfying the assumption of independent and identically distributed (i.i.d.) errors. The null hypothesis of the test is $H_0: \theta = 1$, indicating that the asset price series follows a random walk process. The alternative hypothesis $H_1: \theta > 1$ suggests that the price series exhibits explosive upward movements, indicating the presence of a bubble. The empirical model can be obtained through cointegration transformation of Formula (1):

$$\Delta P_t = \alpha_{r_1, r_2} + \beta_{r_1, r_2} P_{t-1} + \sum_{i=1}^k \varphi_{r_1, r_2}^i \Delta P_{t-i} + \varepsilon_t \quad (2)$$

In this case, the unit root hypothesis transformation is $H_0: \beta_{r_1, r_2} = 0$, and $H_1: \beta_{r_1, r_2} > 0$. Here, k represents the lag order, r_1 denotes the recursive starting point, and r_2 denotes the recursive endpoint. Let r_w represent the optimal rolling window, expressed as a proportion of the total sample, and satisfying $r_w = r_2 - r_1$, with r_0 as the initial window size. The ADF statistic can be expressed as follows at this point:

$$ADF_{r_1, r_2} = \beta_{r_1, r_2} / \text{se}(\beta_{r_1, r_2}) \quad (3)$$

The ADF statistic is fixed with r_1 at the beginning of the test sequence and with r_2 at the end of the test sequence. The GSADF statistic has a more flexible window, calculating all possible ADF values and taking the maximum value as the GSADF statistic, provided the minimum window width requirement is met. The BSADF method fixes r_2 at the endpoint of the sequence and, while ensuring the minimum window width, continuously changes the starting position backward to calculate the corresponding maximum ADF value.

$$GSADF_{(r_0)} = \sup\{ADF_{r_1}^{r_2}\}, r_2 \in [r_0, r_1], r_1 \in [0, r_2 - r_0] \quad (4)$$

$$BSADF_{r_2}(r_0) = \sup\{ADF_{r_1}^{r_2}\}, r_1 \in [0, r_2 - r_0 + 1] \quad (5)$$

After obtaining the GSADF statistic, it needs to be compared with the corresponding critical value simulated at the confidence level to determine the presence of a bubble. The critical value here is obtained through Monte Carlo simulation based on the sample size and the minimum window width. If the GSADF statistic is greater than the critical value, a bubble exists; otherwise, there is no bubble. Once the existence of a price bubble is confirmed, further comparison between the BSADF statistic and the corresponding critical value is needed to determine the timing of the bubble's emergence and collapse. The point at which the BSADF value first exceeds the critical value is marked as the starting point of the bubble, while the point at which the BSADF statistic first falls below the critical value is marked as the collapse point of the bubble.

We selected copper, aluminum, lead, zinc, and nickel, which are high in production and widely used in China, as the research objects. The price data involved are sourced from the Oriental Wealth Network's Choice Financial Database, comprising price indices for the five major nonferrous metals. The sampling frequency is daily. The sample period spans from January 1, 2019, to December 31, 2023, excluding missing values caused by holidays and other reasons. The effective sample sizes for copper, aluminum, lead, zinc, and nickel are 1210, 1210, 1209, 1189, and 1189, respectively. We utilized the Geopolitical Risk Index (GPR) to measure geopolitical risks, with a sampling frequency of daily data and an effective sample size of 1826.

3 Empirical Analysis

3.1 Diagnosis of Price Bubbles

The initial window width r_0 is set according to Philips' research[11], taken as $(0.01 + 1.8/\sqrt{T}) \times T$, where T represents the sample size. The initial window widths for copper, aluminum, and lead are set to 75, while for zinc and nickel, they are set to 74. Monte Carlo simulation is conducted 1000 times in MATLAB to obtain the critical value cv . Price bubble risks in nonferrous metals are described using "bubble length," "bubble frequency," and "bubble intensity." "Bubble length" refers to the total duration of bubbles during the study period; "bubble frequency" indicates the number of bubble occurrences during the study period, with the shortest bubble duration set at 3 days according to Etienne's viewpoint[12]; "bubble intensity" represents the longest duration of bubbles during the study period. The BSADF statistic (5) are used to determine the duration of bubbles.

Table 1 reports the statistical characteristics of price bubbles for the five types of nonferrous metals. The test results show that, at a 95% confidence level, copper, aluminum, zinc, and nickel all exhibit price bubbles. However, the GSADF value for lead price series is 1.726, which is less than the critical value of 2.42, indicating that the phenomenon of price bubbles in lead is not significant. From Table 1, it can be observed that from 2019 to 2023, the price bubble duration for copper is 115 days, and for nickel it is the shortest at 47 days. Regarding bubble frequency, there is little difference among the price bubble frequencies of various nonferrous metals. In terms of bubble intensity, aluminum has the highest intensity, with the longest bubble duration of 52 days; the lowest intensity is observed in the zinc market, with the longest bubble lasting only 26 days. In the indicator system characterized by the length, frequency, and intensity of price bubbles, the ranking of price bubble risks in nonferrous metals market from high to low is aluminum > copper > zinc > nickel.

Table 1. Results of Price Bubble Existence Test and Feature Extraction in Nonferrous Metal Prices.

Variety	GSADF Value	95%CV	Existence of Bubble	bubble length	bubble frequency	bubble intensity
copper	4.427	2.448	YES	115**	5	37
aluminum	3.408	2.448	YES	103	6**	52**
zinc	6.229	2.442	YES	61	5	26*
nickel	4.888	2.442	YES	47*	4*	31
lead	1.726	2.420	NO			

3.2 Contagion of Price Bubbles

Further analyze the causal relationships between the price bubbles of the four nonferrous metals based on the identification of price bubbles in nonferrous metals. The testing steps are as follows: first, test the stationarity of the BSADF sequences of nonferrous metal prices; if the BSADF sequence is stationary, establish a VAR model; if the BSADF sequence is non-stationary, establish a VEC model; then, study the contagion between price bubbles of nonferrous metals through Granger causality tests or cointegration analysis. Unit root tests show that the BSADF sequences of copper, aluminum, zinc, and nickel prices are stationary sequences. The optimal lag order of the VAR model is determined based on the principle of minimizing AIC and SC values, and it is found to be 5. Table 2 reports the results of Granger causality tests based on the VAR model.

Table 2. Results of Granger Causality Test for Nonferrous Metal Price Bubbles

H0	p	result	H0	p	result
Cu does not granger cause Al	0.000	refuse	Al does not granger cause Ni	0.001	refuse
Al does not granger cause Cu	0.372	accept	Ni does not granger cause Al	0.652	accept
Cu does not granger cause Ni	0.001	refuse	Al does not granger cause Zn	0.000	refuse
Ni does not granger cause Cu	0.477	accept	Zn does not granger cause Al	0.014	accept
Cu does not granger cause Zn	0.000	refuse	Zn does not granger cause Ni	0.231	accept
Zn does not granger cause Cu	0.686	accept	Ni does not granger cause Zn	0.929	accept

Establish an R-Vine Copula model to explore the contagion relationships among non-ferrous metal price bubbles. The specific steps are as follows: Determine the optimal lag order of each futures price bubble series according to the criterion of minimum AIC. Model the marginal distribution of each metal bubble using ARMA(p,q)-GARCH(1,1)-skewed t distribution. Conduct LB and LM tests on the modeled series, and the test results indicate that the series do not exhibit heteroscedasticity and have autocorrelation. Establish the static dependence structure of price bubbles among the metals using the R-Vine Copula model. Determine the optimal RVM based on the maximum spanning tree principle, select the best Copula type for each connected node according to the criteria of maximum likelihood function value and minimum AIC value, and estimate the parameters. The entire process is implemented in RStudio. This paper only uses the first tree to describe the static dependence relationship among the futures. Due to space limitations, the specific RVM matrix, parameter estimation matrix, and the dependence structures of other trees for commodity price bubbles during the study period are not provided. The arrows indicate the direction of Granger causality at the 5% confidence level. The letters above the connecting lines represent the type of Copula, and the numbers in parentheses indicate the dependency relationship.

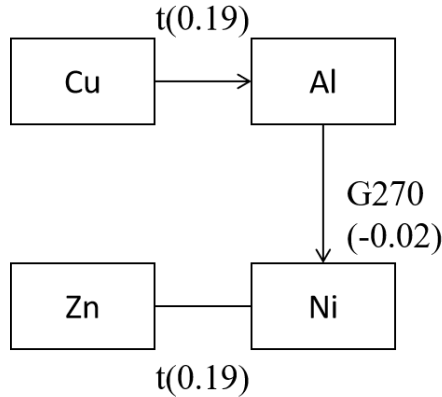


Fig. 1. The contagion structure of non-ferrous metal price bubbles.

Figure 1 reports the contagion structure of non-ferrous metal price bubbles. The test results indicate that the price bubble in copper is a Granger cause for the price bubbles in aluminum, zinc, and nickel, meaning that a price bubble in copper will trigger price bubbles in aluminum, zinc, and nickel. The price bubble in aluminum is a Granger cause for the price bubbles in zinc and nickel, and there is a bidirectional Granger causality between aluminum and zinc. When a price bubble occurs in the aluminum market, it will lead to price bubbles in the zinc and nickel markets. Similarly, a price bubble in the zinc market will also lead to a price bubble in the aluminum market. This structure indicates that copper price bubbles are of high importance among non-ferrous metals.

3.3 Response to External Shocks

Using the VAR model to analyze the impact of international geopolitical risk on the price bubbles in the domestic nonferrous metals market. Unit root tests indicate that the geopolitical risk index is a stationary series. Separate VAR models were established for the international geopolitical risk and the price bubbles of four domestic nonferrous metals: copper, aluminum, zinc, and nickel. The optimal lag orders for the four VAR models, determined based on the principle of minimizing AIC and SC values, are 14, 21, 14, and 16, respectively. The results of the Granger causality test between geopolitical risk and the four metals indicate that, at the 5% significance level, international geopolitical risk is a Granger cause of the price bubble series for domestic copper and aluminum. Additionally, there is no significant Granger causality between geopolitical risk and the price bubble series for domestic zinc and nickel. The impulse response analysis of the price bubbles for copper and aluminum was conducted using the VAR model.

Figure 2 reports the impulse response results of copper and aluminum price bubbles to geopolitical risk shocks. The results show that after a positive shock of one standard deviation in international geopolitical risk, the prices of domestic copper and aluminum

experience a significant upward trend, with the price bubbles gradually expanding. The positive response persists for the first 8 trading days following the shock. The response value reaches its peak on the 6th trading day after the shock, stabilizes by the 9th trading day, and gradually weakens to zero.

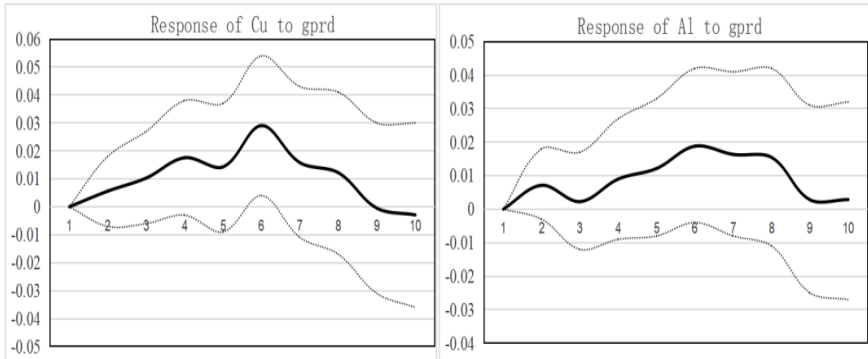


Fig. 2. Results of Nonferrous Metal Price Bubbles' Impulse Response to Geopolitical Risk.

4 Conclusions

This study, based on price data from 2019-2023, the BSADF method, and the VAR model, identified the statistical characteristics, contagion, and impulse responses to international geopolitical risks of price bubbles in five major nonferrous metals in China. The following conclusions were drawn: 1. Significant price bubbles exist in the domestic markets for copper, aluminum, zinc, and nickel, whereas the price bubble in lead is not significant. The price bubbles in China's nonferrous metals market are predominantly long bubbles. The risk ranking of price bubbles in nonferrous metals from highest to lowest is aluminum, copper, zinc, and nickel. 2. In terms of the contagion path of price bubbles, a price bubble in the domestic copper market will trigger price bubbles in aluminum, zinc, and nickel. A price bubble in the aluminum market will trigger price bubbles in zinc and nickel, and a price bubble in the zinc market will trigger a price bubble in aluminum. It is important to monitor the price bubbles in copper and aluminum markets closely. 3. International geopolitical risks impact the domestic markets for copper, aluminum, and other nonferrous metals, potentially leading to price bubbles. Therefore, it is crucial to guard against the risks of price bubbles in nonferrous metals induced by geopolitical events.

Acknowledgements

Supported by the Jiangxi Province Key Research Base Project in Philosophy and Social Sciences (Project Number: 23ZXSKJD04), Jiangxi Province University Key Research Base Tender Project in Humanities and Social Sciences (Project Number: JD20005).

References

1. Li Jian, Lü Jie, Li Chongguang. Real-time Early Warning Research on Bubble Risk in Agricultural Product Futures Market [J]. *China Rural Economy*, 2019, (03): 53-64. DOI:CNKI:SUN:ZNJJ.0.2019-03-004.
2. Ming Lei, Wu Yifan, Xiong Xiong, et al. Bitcoin Price Bubble Test, Evolution Mechanism and Risk Prevention [J]. *Economic Review*, 2022, (1): 96-113. DOI:10.19361/j.er.2022.01.07.
3. Lin Sihan, Chen Shoudong, Wang Yan. Research on the Asymmetric Dynamic Impact of China's Macro Leverage Ratio on Real Estate Price Bubbles [J]. *Financial Review*, 2021, 13(05):91-105+125-126.
4. un. Investor Sentiment, Stock Liquidity, and Stock Price Bubbles: An Analysis Based on GASDF Test Method [J]. *Operations Research and Management*, 2023, 32(07): 156-161. DOI:10.12005/orms.2023.0231.
5. Xu Le, Zhao Lingdi. Research on Speculative Bubble Risk of Nonferrous Metal Futures Prices: An Empirical Analysis Based on GSADF Method [J]. *Price Theory and Practice*, 2018, (12): 119-122. DOI:10.19851/j.cnki.cn11-1010/f.2018.12.027.
6. Yang Yanjun, Tang Di. Real-time Early Warning Research on Price Bubbles in China's Nonferrous Metal Futures Market: An Analysis Based on the Supremum ADF Test Method [J]. *Price Theory and Practice*, 2022, (12): 114-117. DOI:10.19851/j.cnki.cn11-1010/f.2022.12.400.
7. Lin Xuegui. Spillover Effect of Cotton Price Fluctuation [J]. *China Management Science*, 2016, 24(S1): 504-508. DOI: CNKI:SUN:ZGGK.0.2016-S1-072.
8. Liu Huajun, Chen Minghua, Liu Chuanming, et al. Network Structure and Dynamic Interactive Effects of China's Commodity Prices Spillover [J]. *Journal of Quantitative & Technical Economics*, 2017, 34(01): 113-129. DOI:10.13653/j.cnki.jqte.2017.01.007.
9. Li Lunyi, Zhang Xiang. Price Bubbles and Spatial Contagion Effects in China's Real Estate Market [J]. *Journal of Financial Research*, 2019, (12): 169-186. DOI:CNKI:SUN:JRYJ.0.2019-12-010.
10. Guo Wenwei. Research on the Contagion Mechanism of Domestic and Foreign Commodity Price Bubbles [J]. *Journal of Central University of Finance and Economics*, 2022, (4): 37-49. DOI:10.19681/j.cnki.jcufe.2022.04.007.
11. Phillips P C B, Shi S, Yu J. Testing for multiple bubbles: Historical episodes of exuberance and collapse in the S&P 500[J]. *International economic review*, 2015, 56(4): 1043-1078. <https://doi.org/10.1111/iere.12132>.
12. Etienne X L, Irwin S H, Garcia P. Bubbles in food commodity markets: Four decades of evidence[J].*Journal of International Money and Finance*,2014,42(4):129-155. <https://doi.org/10.1016/j.jimonfin.2013.08.008>.

Open Access This chapter is licensed under the terms of the Creative Commons Attribution-NonCommercial 4.0 International License (<http://creativecommons.org/licenses/by-nc/4.0/>), which permits any noncommercial use, sharing, adaptation, distribution and reproduction in any medium or format, as long as you give appropriate credit to the original author(s) and the source, provide a link to the Creative Commons license and indicate if changes were made.

The images or other third party material in this chapter are included in the chapter's Creative Commons license, unless indicated otherwise in a credit line to the material. If material is not included in the chapter's Creative Commons license and your intended use is not permitted by statutory regulation or exceeds the permitted use, you will need to obtain permission directly from the copyright holder.

